Permanent-Magnet Synchronous Generator Supplying an Isolated Load

T. F. Chan[1], Weimin Wang[1], and L. L. Lai[2]
[1]Department of EE, The Hong Kong Polytechnic University, Hung Hom, Hong Kong, China
[2]Energy Systems Group, School of Engineering and Mathematical Sciences, City University London, UK
eetfchan@polyu.edu.hk

***Abstract* — The steady-state and transient performance of a surface-inset permanent-magnet synchronous generator (PMSG) feeding an isolated load is studied using a coupled-circuit, time-stepping, two-dimensional finite-element analysis. Nonlinearities in the field and electric circuit are taken into consideration and both passive ac load and bridge rectifier dc load operating conditions are analyzed. The main contribution of this paper is the quantitative analysis of voltage and current harmonics, as well as the study of short-circuit performance. The computed results have been verified by experiments on a 2.5 kVA generator.**

I. Introduction

Permanent-magnet synchronous generators (PMSGs) are increasingly used for distributed generation and many stand-alone applications. For these applications the PMSG may supply a passive R-L load or a dc load via a diode bridge rectifier connected across the armature terminals [1]. The nonlinear electric and field systems pose considerable difficulties in analysis. In this paper, a time-stepping, coupled field-circuit finite element method [2], [3] is used for performance analysis of a surface-inset PMSG feeding an isolated load. Besides the field characteristics, the coupled field-circuit solution also yields other useful generator information, taking into consideration the armature current effect, magnetic saturation, and circuit nonlinearities. The analysis result helps in improving the generator design aspects. The computed results have been verified by experiments on a 2.5 kVA generator.

II. Analysis

The electric circuit of a star-connected PMSG that supplies a three-wire R-L load comprises six circuit variables, namely the resultant generated phase EMFs e_A, e_B, and e_C and the phase currents i_A, i_B and i_C. The external circuit comprises the armature resistance R, armature end-winding leakage inductance L_e, and the load impedance. In the case of a PMSG supplying a bridge rectifier load (Fig. 1), the additional circuit components include the six diodes D_1 to D_6, the load resistance R_L, and the load inductance L_L. In the present FEA study the field-circuit coupling is accomplished via the phase EMFs e_A, e_B, and e_C, each of which being the sum of the e.m.f.s of all the coil-sides that make up the phase winding. The field region occupied by a coil-side has vector potential, current and EMF degrees of freedom (DOFs). The circuit element that represents the corresponding coil-side has three nodes (I_i, J_i, K_i). I_i and J_i are the negative and positive nodes that have the Voltage degrees of freedom, and each of these nodes is connected to that of the adjacent coil sides, depending upon the winding configuration. The third node K_i is a selected node in the conductor field region and it has both current and EMF degrees of freedom. Since all the current and back EMF variables in the conductor field region have already been unified, the vector potentials of all these nodes will be used to evaluate the back EMF and current to be returned to node K_i. The field region and the corresponding circuit component are thus coupled together. Each phase winding can now be constructed by connecting the appropriate circuit elements. Finally, the external circuit for isolated operation of the three-phase AFPMSG is set up by including the load impedances.

In the case of a rectifier load, the actual circuit configuration depends upon the conduction states of the diodes, which are conveniently modelled by their Norton equivalent circuits. Each diode is represented by a piecewise-linearized current-voltage curve, defined by the forward voltage, forward resistance and the reverse blocking resistance.

Maxwell's equations, applied to PMSG domains, will give rise to the diffusion equations:

$$\begin{aligned} &\nabla\times(\nu\nabla\times A)=0, && \text{in iron and air gap}\\ &\nabla\times(\nu\nabla\times A)=\frac{i_s}{S}, && \text{in armature windings}\\ &\nabla\times(\nu_{PM}\nabla\times A)=\nabla\times(\nu_{PM}B_r), && \text{in permanent magnets}\end{aligned} \quad (1)$$

where A, ν, i_s, S, B_r and ν_{PM} are magnetic vector potential, reluctivity, armature phase current, total cross-sectional area of one turn, remanent flux density of the PM and equivalent reluctivity, respectively.

By applying periodic conditions, the solution region can be confined to a half cross-section of the PMSG (Fig. 1). In this work, a time-step corresponding to two mechanical degrees of rotor movement was found to give satisfactory results without unduly long computation time.

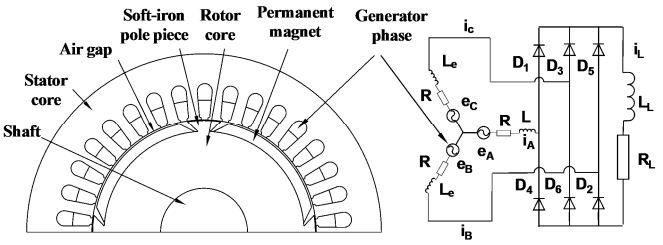

Fig. 1. Cross-section of prototype PMSG with inset rotor construction feeding a rectifier load

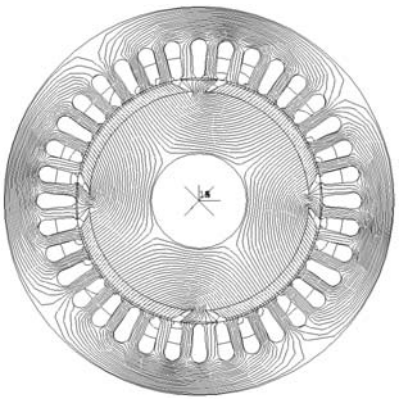

Fig. 2. Cross-section of PMSG with surface-inset rotor and the flux plot obtained from FEA

The time-stepping, coupled field-circuit, 2-D FEA was performed in order to study the steady-state and transient performance of the experimental PMSG with surface-inset rotor [3]. Constant speed operation is assumed and the PMSG supplies an isolated load. Both passive load and rectifier load cases are analyzed. Fig. 2 shows the cross-section of the machine and the field plot obtained.

III. GENERATOR PERFORMANCE

A. PMSG Supplying an Isolated Passive Load

Fig. 3 shows the computed and experimental waveforms of the PMSG on no load and Fig. 4 shows the computed and experimental waveforms of phase voltage and phase current when the PMSG is supplying a load resistance of 9.1 Ω per phase. It is observed that the waveforms computed from FEA match the experimental waveform very closely, thus verifying the validity of the field computation method. It is found that there is marked distortion in the phase voltage waveform when the PMSG is on load. To study the effect of load current on the harmonics, a harmonic analysis was carried out on the waveforms computed from FEA. From Fig. 5, it is seen that both the 3rd and 15th harmonics increase with load current, while the 9th triplen harmonics remains constant. On the other hand, the non-triplen harmonics mostly decrease with increase in load current. It can be concluded that the increased harmonic distortion in phase voltage is due to increase in the triplen harmonics. Since a three-wire load is being supplied, the current waveform in Fig. 4 is practically sinusoidal since triplen harmonics are suppressed across the lines. On no load, the total harmonic distortion (THD) in the phase voltage and line voltage is 5.3% and 3.45%, respectively. At full load (13 A), the THD in the phase voltage is 9.4 %, whereas THD in the line voltage (and load current) is only 2.5%.

B. Transient Switching of Isolated Passive Load

The time-stepping coupled field-circuit method was next used to study the transient performance of the PMSG. The PMSG was operating on no-load at rated speed when a balanced resistive load of 12.45 Ω per phase was switched across the generator terminals. As shown in Fig. 6, a brief transient period follows the application of load at time t = 1.018 s, and a notch is produced in the voltage waveform. Agreement between the computed and experimental waveforms is good in general, but the deviation in frequency becomes more pronounced due to the speed drop in the experimental machine set, a fact which was not accounted for in the FEA.

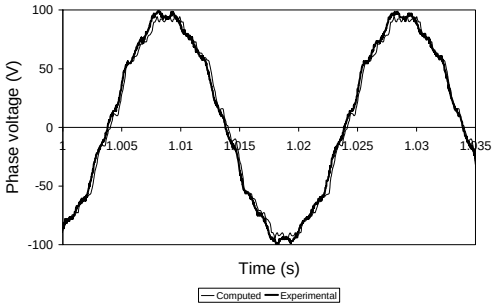

Fig. 3. Computed and experimental waveforms of no-load phase voltage

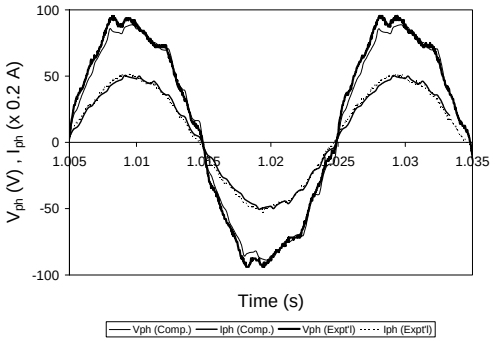

Fig. 4. Computed and experimental waveforms of phase voltage and phase current when the PMSG is supplying a load resistance of 9.1 Ω per phase

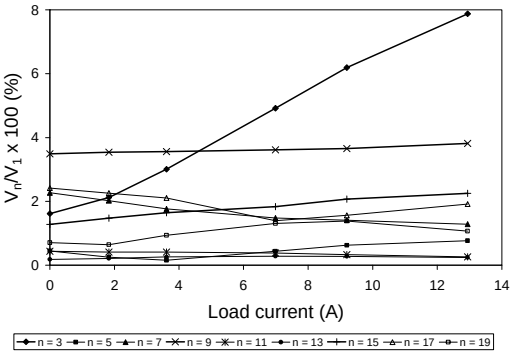

Fig. 5. Computed harmonics in the phase voltage when the PMSG is supplying a resistive load

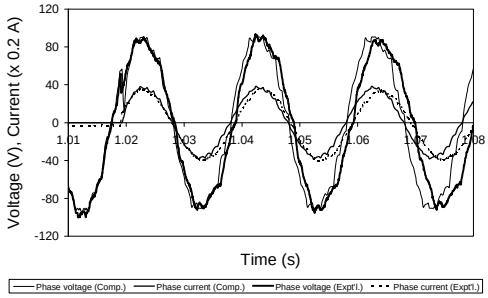

Fig.6. Waveforms of phase voltage and phase current when a load resistance of 12.45 Ω per phase is switched across the generator terminals

C. *Short-circuit Transients*

The time-stepping coupled field-circuit method was also used for studying the short-circuit performance of the PMSG and the computed results are shown in Fig. 7. The PMSG is assumed to be running on open circuit when a three-phase short circuit occurs at the terminals. Since triplen harmonic currents cannot flow, the triplen harmonic voltage components remain in each phase during the short circuit (Fig. 7). The steady-state short-circuit current, however, is quite sinusoidal as observed from Fig. 8. The peak short-circuit current reaches 131 A, while the steady-state short-circuit current is 107 A (peak), or 76 A (rms), which is almost six times the rated current.

Fig. 9 shows the distribution of the normal flux density at the mean air gap of the PMSG computed at the instant when maximum short-circuit current (131 A) is flowing. Due to the inset rotor construction, the flux density is large in the interpolar regions (I) where the soft iron rotor pole pieces are located. Over the surfaces of magnets (II), however, the flux density is smaller due to the demagnetizing effect of the armature currents.

Fig. 10 shows the computed flux density distribution at different radial positions of a rotor magnet at the same time instant. It is observed that there are regions in the rotor magnet with flux reversal, i.e., flux density less than zero. This implies that partial demagnetisation in the magnet will result subsequent to a terminal three-phase short circuit.

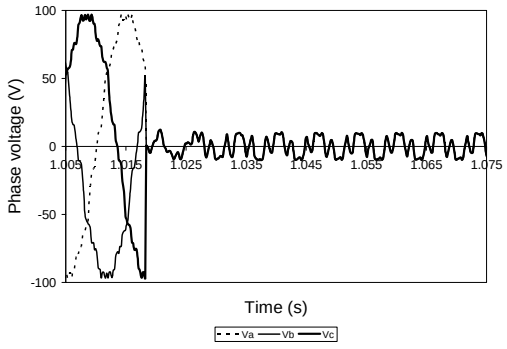

Fig. 7. Three-phase short-circuit transients of PMSG: phase voltage waveforms

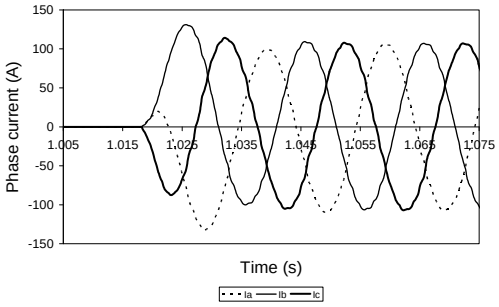

Fig. 8. Three-phase short-circuit transients of PMSG: phase current waveforms.

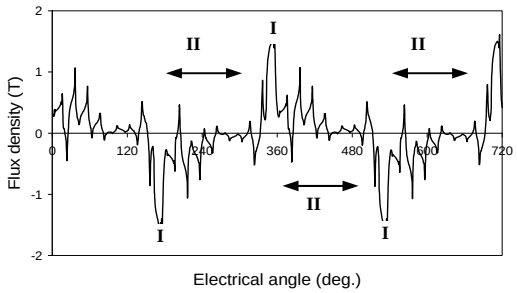

Fig. 9. Computed air gap flux density distribution of PMSG when phase A is carrying maximum instantaneous short-circuit current (I: interpolar regions; II: surfaces of magnets)

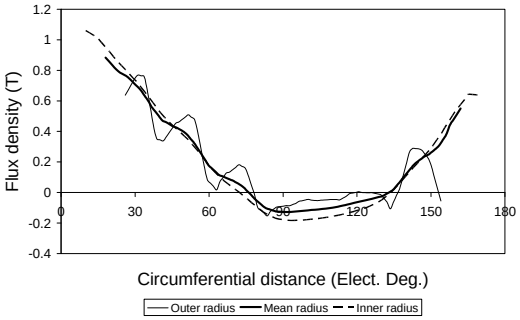

Fig. 10. Computed flux density at different radial positions of a rotor magnet when phase A is carrying maximum instantaneous short-circuit current

D. *PMSG Supplying a Rectifier Load*

Fig. 11 shows the computed and experimental phase voltage waveforms of the PMSG-rectifier-load system when R_L = 9.2 Ω and L_L = 0. Compared with the waveforms for passive loads (Fig. 4), the harmonic distortion the phase voltages and phase currents is more severe due to the nonlinear load. During commutation overlap, the phase voltage is approximately constant at 50 V while the phase current increases (or decreases) approximately linearly, giving rise to quasi-trapezoidal current pulses in the positive and negative half cycles (Fig. 12). The good agreement between computed and experimental waveforms confirms the validity of the coupled field-circuit FEA as applied to a PMSG supplying rectifier loads.

Fig. 13 shows the variation of voltage harmonics with load current of the PMSG from a Fourier analysis of the computed waveforms. It is found that variation of the triplen harmonics is practically the same as that for the passive load case. The variation of non-triplen harmonics, however, shows a great difference. The predominant harmonic is the 5th, and it increases rapidly with load current. As a result the THD in the line voltage also increases with load.

Fig. 14 shows the corresponding variation of harmonics in the phase current. The harmonic contents are large as a result of the nonlinear rectifier load. All the triplen harmonics are absent, while most of the harmonics decrease as the load current increases. The THD in the phase current drops from 27% to 20.6% as the load current increases from 2.8 A to 11.7 A.

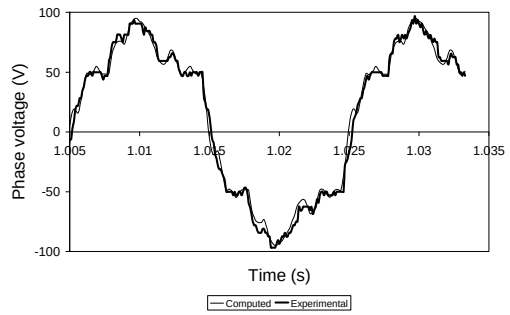

Fig. 11. Waveforms of phase voltage when the PMSG is supplying a rectifier load (R_L = 9.2 Ω)

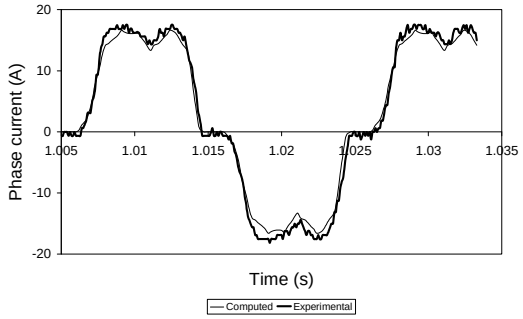

Fig. 12. Waveforms of phase current when the PMSG is supplying a rectifier load (R_L = 9.2 Ω)

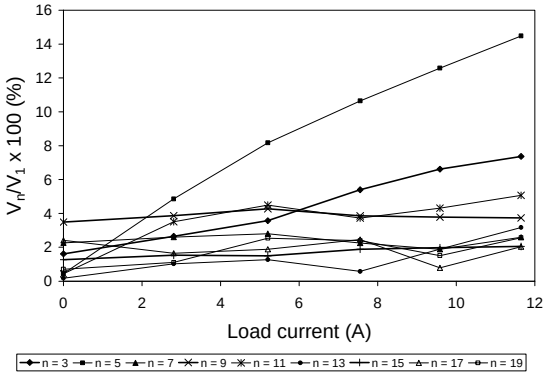

Fig. 13. Computed harmonics in the phase voltage when the PMSG is supplying a rectifier load

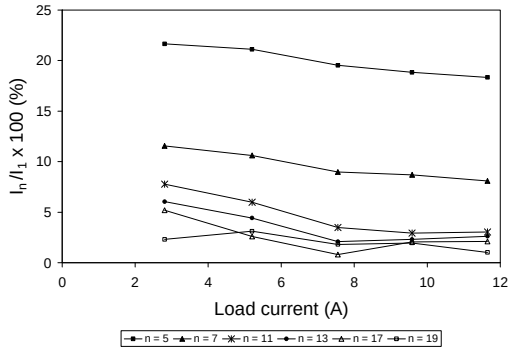

Fig. 14. Computed harmonics in the phase current when the PMSG is supplying a rectifier load

Fig. 15 shows the computed and experimental waveforms of the phase current when R_L = 9.2 Ω and L_L = 11.27 mH. Compared with the waveforms in Fig. 12 (when there is no filter inductance), the ripple content in the phase current (and hence the dc load current) is reduced considerably. A filter inductance L_L in series with R_L in the circuit shown in Fig. 1 is thus useful in improving the quality of the output current.

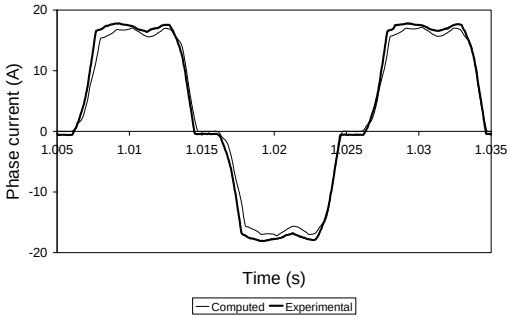

Fig. 15. Computed and experimental waveforms of phase current when the PMSG is supplying a rectifier load (R_L = 9.2 Ω, L_L = 11.27 mH)

IV. CONCLUSIONS

In this work, the performance analysis of a permanent-magnet synchronous generator with inset rotor feeding an isolated load using a coupled-circuit, time-stepping, 2-D FEM is described. The direct-coupled field-circuit method enables the instantaneous value of field and circuit variables to be solved simultaneously without using the D-Q axis model of the generator. Both steady-state and transient operation of the PMSG can be analyzed. PMSG supplying a rectifier load can also be handled. A short-circuit study reveals regions of the rotor permanent magnet that might suffer from partial demagnetization. Based on waveforms computed from FEA, a quantitative analysis of the harmonics and THD of a PMSG is also presented and interesting results have been obtained for both passive load and rectifier load. The computed results are validated through measurements on a 2.5 kVA prototype generator.

V. ACKNOWLEDGMENT

The work described in this paper was fully supported by a grant from the Research Grants Council of the Hong Kong Special Administrative Region, China (Project No. PolyU 5121/06E).

VI. REFERENCES

[1] O. Ojo and J. Cox, "Investigation into the performance characteristics of an interior permanent magnet generator including saturation effects," in *Conf. Rec. 1996 IAS Annual* Meeting, vol. 1, pp. 533-540.

[2] S. Williamson and A. F. Volshenk, "Time-stepping finite-element analysis for a synchronous generator feeding a rectifier load," *IEE Proc.—Elect. Power Appl.*, 142(1): 50–56, 1995.

[3] T. F. Chan, L. L. Lai and L. T. Yan, "Analysis of a stand-alone permanent-magnet synchronous generator using a time-stepping coupled field-circuit method," *IEE Proc.–Elect. Power Appl.*, 152(6): 1459-1467, 2005.